Supporting Information

Self-assembling two-dimensional nanophotonic arrays for reflectivity-based sensing

Ye Ma[1,2], Debabrata Sikdar[1,3], Qian He[4], Daniel Kho[1], Anthony R. Kucernak[1], Alexei A. Kornyshev[1], Joshua B. Edel[1]

[1]Department of Chemistry, Imperial College London, Molecular Science Research Hub, White City Campus, 80 Wood Lane, W12 0BZ, UK
[2]School of Materials Science and Engineering, Ocean University of China, Qingdao, 266100, China
[3]Department of Electronics and Electrical Engineering, Indian Institute of Technology Guwahati, Guwahati-781039, India
[4]Key Lab of Marine Chemistry Theory & Technology, Ministry Education, Ocean University of China, Qingdao, 266100, China

[Correspondence: Joshua.Edel@imperial.ac.uk , A.Kornyshev@imperial.ac.uk , A.Kucernak@imperial.ac.uk]

Table of contents

1. TEM and diameter of NPs

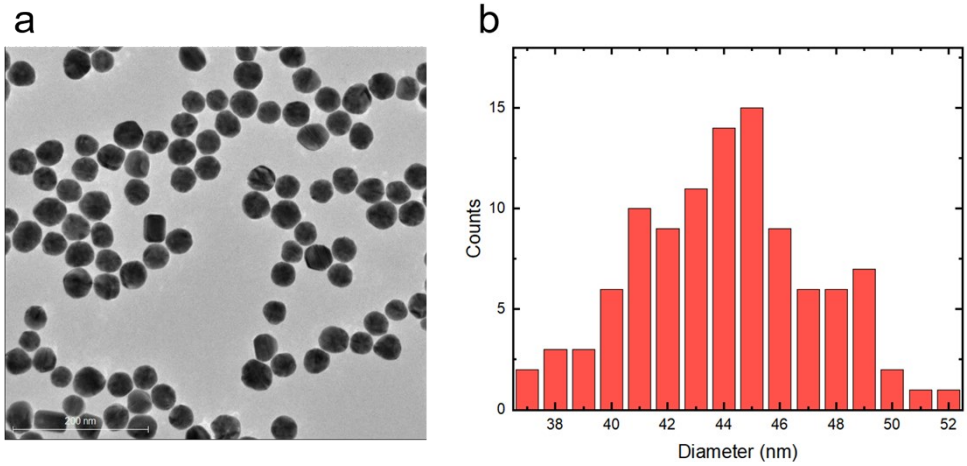

Figure S1*. (a) Transmission electro-microscope (TEM) image of 44±3 nm Au nanoparticles used in this study. (b) Statistics of NP diameter measured from TEM images using ImageJ.*

2. GSH functionalization and lead-induced aggregation in the bulk solution

A careful study of GSH NP behaviour in the bulk is crucial for understanding how this NP system will function. To secure the stability of GSH-NP solution, we keep the pH of all the samples above 6, GSH concentration as 10 µM and centrifugation speed at 1500 rcf (relative centrifugal force). The comparison of UV-vis spectra between the citrate and GSH functionalized NPs before/after adding lead (**Figure S3**) concludes: only GSH functionalized NPs aggregate in the presence of lead. Employing dynamic light scattering (DLS), we examined the hydrated diameter of citrate or GSH functionalized NPs before/after adding lead. Revealed in **Figure S4**, the hydrated diameters of both citrate and GSH functionalized NPs are around 50 nm in the absence of lead. As expected, by adding 2 ppb lead, the output for citrate NPs stays unchanged while the GSH NPs give larger averaged diameter (100 nm) and broader distribution, further confirming the anchoring of GSH on NPs and the specific bonding between lead and GSH. DLS measurements were performed on a Delsa Nano C particle analyser (Beckman Coulter, USA).

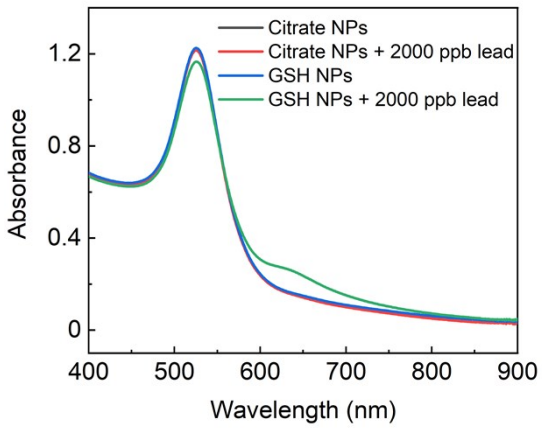

Figure S2*. UV-vis spectra of Citrate- or GSH-functionalized Au NPs with 2000 ppb lead ions in the bulk solution and without any presence of lead*

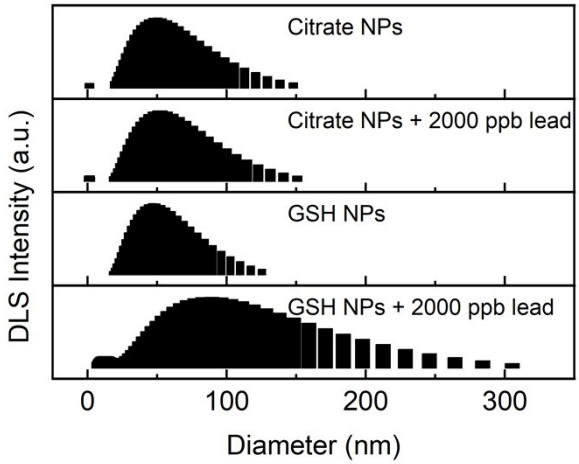

***Figure S3**. DLS measurements of the responses of citrate or GSH functionalized NPs to 2000 ppb lead: only GSH NPs aggregate when lead exists. From top to bottom: Citrate NPs without lead, citrate NPs with 2000 ppb lead, GSH NPs without lead, GSH NPs with 2000 ppb lead.*

3. Quantitative detection of lead in the bulk

For the detection of lead-ions in the bulk solution, lead ions were added into the GSH-NP solution at pH 8 to reach the designated final concentrations. After 1 min shaking and 10 min settling, the samples are examined through UV-vis.

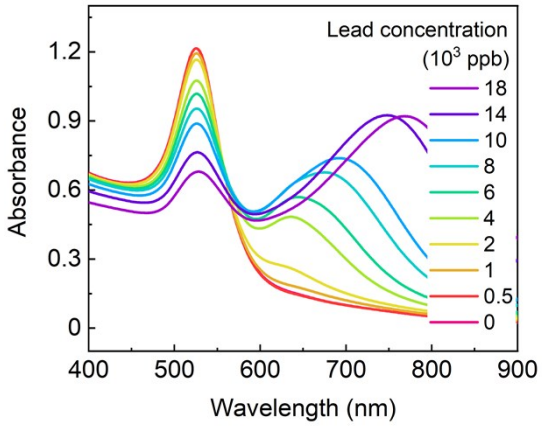

***Figure S4**. UV-vis spectra of GSH NPs bulk solution with different concentrations of lead (0, 500, 1000, 2000, 4000, 6000, 8000, 10000, 14000, 18000 ppb).*

4. The influence of GSH concentration during the NP functionalization

Based on GSH taking up approximately 0.189 nm^2,[1] the maximum coverage of GSH on 44 nm NPs is 3.2×10^4. Based on the initial GSH concentration used the GSH:NP ratio was 8.8×10^4 which is more than enough for complete coverage of the NP.

Experiments were also performed to demonstrate the effect of GSH concentration on the sensor. After adding 150 ppb lead, we compared the reflectance spectra of the NP assemblies with different GSH concentrations during the NP functionalization. As can be seen from Figure S5, there is a minor difference between the samples with 10^{-4} M, 10^{-5} M, 10^{-6} M GSH, while the sample with 10^{-7} M GSH

shows a much weaker reflectance. The reason that we did not use a too high concentration of GSH is that the NPs tend to aggregate during centrifugations, which may be due to the hydrogen bonds between GSH molecules.[2]

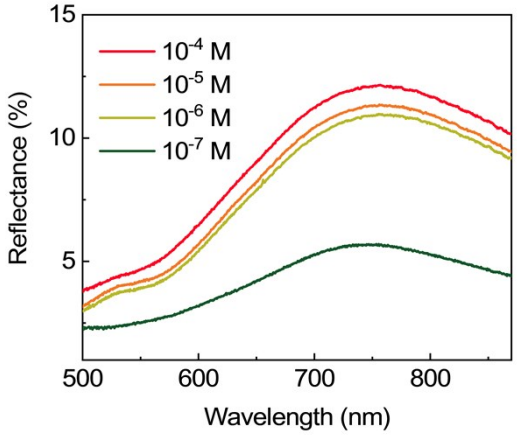

***Figure S5**. The influence of GSH concentration during the functionalization of NPs. Reflectance spectra are shown at a GSH concentration of 10^{-4} M, 10^{-5} M, 10^{-6} M or 10^{-7} M respectively. The lead concertation was kept constant at 150 ppb in all cases.*

5. The effect of pH on lead detection in the bulk solution

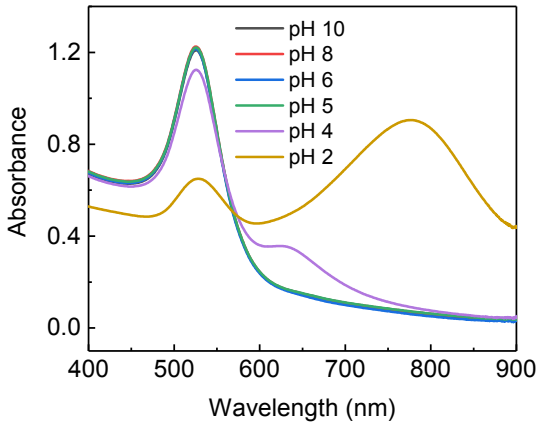

***Figure S6**. UV-vis spectra of the bulk solution of GSH Au NPs at different pH.*

6. Influence on spectra in the presence of Hg(II)

We compared the reflectance spectra of 400 ppb Hg(II); 200 ppb Pb(II) and 400 ppb Hg(II) + 200 ppb Pb(II) samples (Figure S7). The co-existing of high concentration of Hg(II) can result in a slight increase in the reflectance maxima.

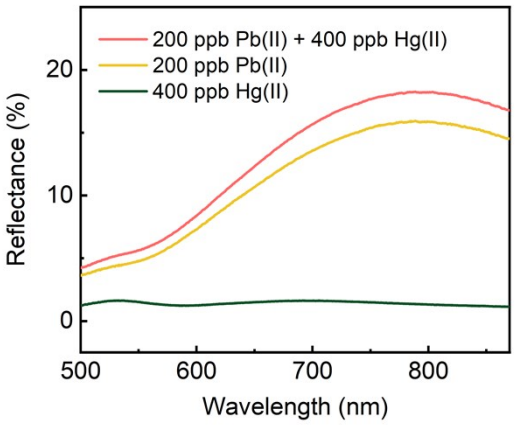

Figure S7. *The reflectance spectra at the LLI of the samples with 400 ppb Hg(II); 200 ppb Pb(II) and 400 ppb Hg(II) + 200 ppb Pb(II). The coexistence of high concentration of Hg(II) has minor influence on the reflectance.*

7. Time dependence of forming aggregation in the bulk solution

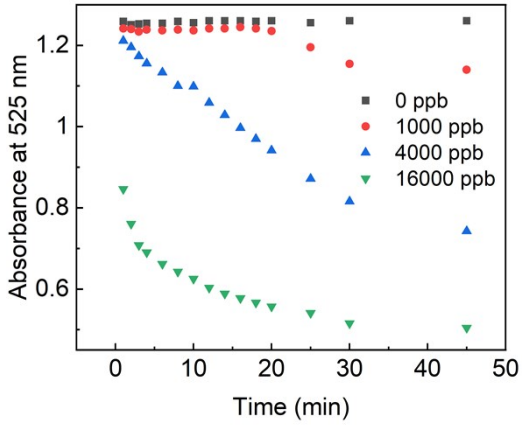

Figure S8. *The time-dependent absorbance of bulk GSH NPs at 525 nm with the presence of 0, 1000, 4000, 16000 ppb lead in the bulk solution.*

8. Increase in surface area and decrease in diffusion time in the LLI system

Assume a vial of internal diameter 2R filled with equal volumes of oil and aqueous phases to a total depth of 2L (i.e. total volume of each phase $V_{oil} = V_{aqueous} = \pi R^2 L$ and interfacial area πR^2). This also assumes that the solutions in the vial are static – i.e. no convection.

If we shake up the two components, we create an oil in water emulsion with droplets of radius, *r*. The total number of droplets

$$N_{droplets} = \frac{V_{oil}}{V_{droplet}} = \frac{\pi R^2 L}{\frac{4}{3}\pi r^3} = \frac{3R^2 L}{4r^3}$$

The ratio of surface areas between all the oil droplets formed upon shaking with the surrounding water and the LLI formed between the two phases before the mixing is

$$\frac{A_{droplets}}{A_{LLI}} = \frac{N_{droplets} 4\pi r^2}{\pi R^2} = \frac{3L}{r}$$

Before we form the droplets the average diffusion distance for NPs dissolved in water to reach its interface with oil is $\frac{L}{2}$. After we form the droplets, we can partition the aqueous phase such that for every droplet of oil, we also have an equivalent volume of surrounding aqueous phase (as the total volumes of both phases are the same). We can then approximate the average diffusion distance as being the extra radius associated with a volume which contains $\frac{3}{2}V_{droplet}$, as this larger volume will contain all of the oil and half the aqueous phase distributed around it. This droplet will have a radius of αr, such that

$$\pi(\alpha r)^3 = \frac{3}{2}\frac{4}{3}\pi r^3$$

$$\alpha = \sqrt[3]{2}$$

So the average diffusion distance is $r(\sqrt[3]{2} - 1)$, and the decrease in diffusion distance is a factor of $\frac{r(\sqrt[3]{2} - 1)}{L/2}$.

Putting in the numbers for the system, R=1cm, L≈3 cm, r≈10μm

The increase in the surface area upon shaking is

$$\frac{A_{droplets}}{A_{LLI}} = \frac{3L}{r} = \frac{3\ 0.03}{10^{-5}} = 9000$$

The ratio of the diffusion distance before mixing to that after mixing is

$$\frac{L/2}{r(\sqrt[3]{2} - 1)} = \frac{0.03/2}{10^{-5}\ 0.26} = 5770$$

i.e. average diffusion distance for nanoparticles is decreased by a factor of ~6000. As diffusion time $t_D \approx \frac{x^2}{2D}$, a decrease in diffusion distance of 5770 leads to a decrease in diffusion time of $(5770)^2 \approx 3.3_X 10^7$ i.e. about 30 million times quicker than a still LLI system.

9. SEM sample preparation for the NP arrays at LLI

Similar to our previous work,[3] a 125 nm thick Au film was deposited through sputter coating (Quorum Tech, Q150T) on a silicon wafer with a 10 nm Titanium interlayer. The substrates were washed vigorously by acetone, ethanol and DI water before and after the deposition. Later, these substrates were soaked into a 1 wt% octane thiol solution in ethanol for 1 hour to form a self-assembled monolayer of octane thiol and washed by ethanol and DI water for later use. The NP array was first formed at the LLI as described in the method part and then transferred to the Au substrate. Initially, 10 ml as GSH Au NPs solution with designated lead concentration was mixed with 4 ml 1,2-dichloroethane in a PTFE jar. After 60 s vigorous shaking on a vortex machine and 60 s settling, the lid was open, allowing the top DCE layer to evaporate. A golden mirror of GSH-NP could be seen atop of the water phase if enough lead is presented. Then a dried Au substrate with octane thiol SAM was carefully stamped onto this NP array and quickly removed from the solution. The substrates then were naturally dried in a fume hood and ready for SEM measurement.

10.Reflectance and UV-vis spectra of high concentration lead in LLI system

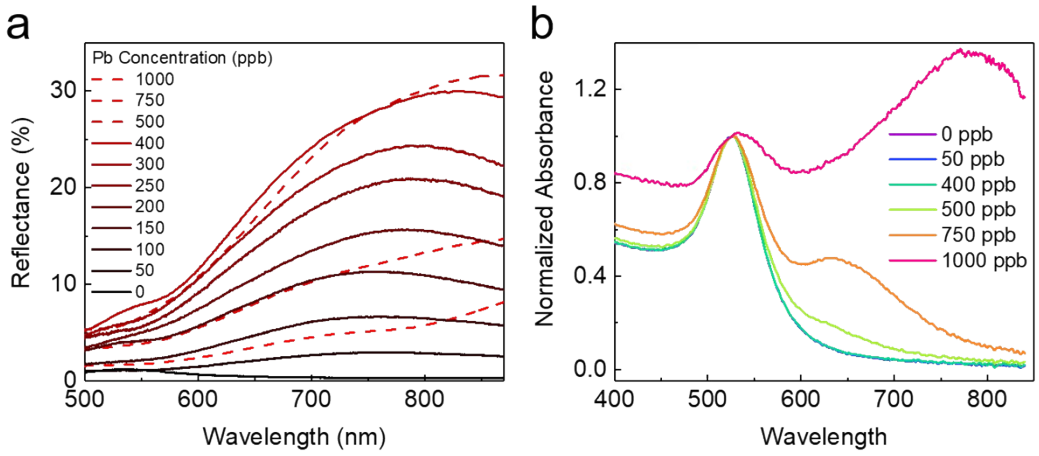

***Figure S9**. a. Reflectance spectra of GSH NPs at the LLI in the presence of 0, 50, 100, 150, 200, 250, 300, 400, 500, 750, 1000 ppb lead in bulk solution. b. Normalized UV-vis absorbance spectra of GSH NP aqueous supernatant in LLI system with 0, 50, 400, 500, 750, 1000 ppb lead.*

11.Reflectance spectra at different points on the LLI

The reflectance spectra at six different points on the LLI were measured (Figure S10). The standard deviation was determined to be less than 0.6 %.

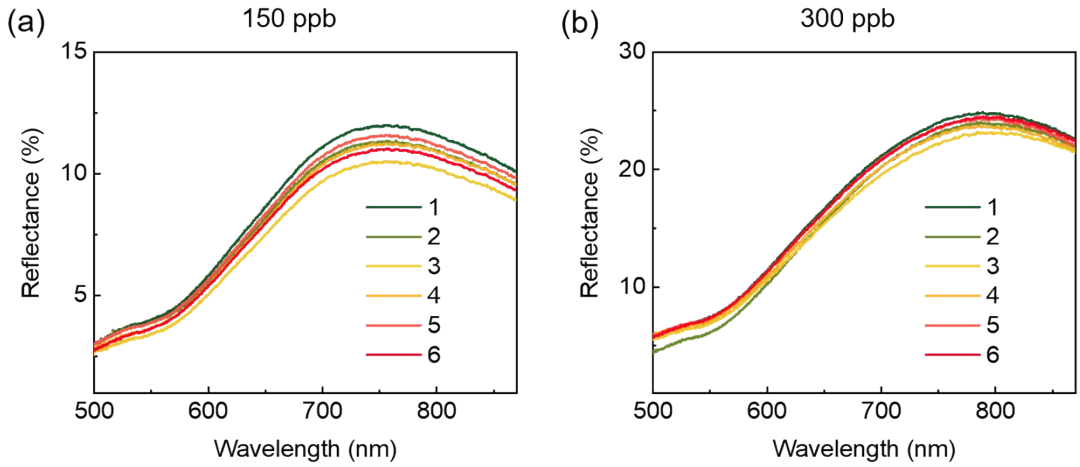

***Figure S10**. Reflectance spectra at six different points on the LLI of the samples with either 150 ppb or 300 ppb lead.*

12. Optical simulations on the monolayer/multilayer structures of the NP array.

We performed additional full-wave simulations (with COMSOL Multiphysics®) to confirm the monolayer structure at the LLI, taking the case of experimentally obtained reflectance curve at 200 ppb as an example. The same structural parameters, such as NP size and interparticle separation are used for obtaining reflectance spectra in case of 1-layer, 2-layers and 3-layers formations during NP

self-assembly, assuming inter-layer gap to be same as the interparticle separation. Figure S11 depicts the comparison between the experimental reflectance curve at 200 ppb with simulated reflectance spectra for 1-layer, 2-layers and 3-layers formations at the LLI. This reveals close correspondence of the experimental curve to the monolayer's spectrum. In case of formation of 2-layers or 3-layers, a dip or a splitting of the resonance peak would have appeared at the long wavelength, as seen in Figure R1, which may be attributed to the absorbance peak arising from modes coupled between the NPs of multiple layers. This was also witnessed in the theoretical study of the multilayer assembly at solid-liquid interfaces.[4] The absence of such dip or peak splitting in our experimental spectrum suggests that there is no multilayer formation.

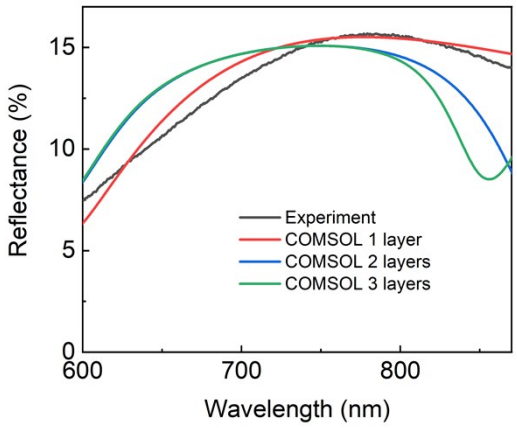

Figure S11. *The experimental reflectance spectrum of the sample with 200 ppb lead (black) and the simulated reflectance spectra with 1 (red), 2 (blue) or 3 (green) layers of NP array at the LLI.*

13.References

1. A. M. Smith, L. E. Marbella, K. A. Johnston, M. J. Hartmann, S. E. Crawford, L. M. Kozycz, D. S. Seferos and J. E. Millstone, *Anal. Chem.*, 2015, **87**, 2771-2778.
2. I. I. S. Lim, D. Mott, W. Ip, P. N. Njoki, Y. Pan, S. Zhou and C.-J. Zhong, *Langmuir*, 2008, **24**, 8857-8863.
3. Y. Ma, D. Sikdar, A. Fedosyuk, L. Velleman, M. Zhao, L. Tang, A. A. Kornyshev and J. B. Edel, *ACS Applied Materials & Interfaces*, 2019, **11**, 22754-22760.
4. D. Sikdar, H. Weir and A. A. Kornyshev, *Optics Express*, 2019, **27**, 26483-26498.